

Dalton Transactions

Accepted Manuscript



This is an *Accepted Manuscript*, which has been through the Royal Society of Chemistry peer review process and has been accepted for publication.

Accepted Manuscripts are published online shortly after acceptance, before technical editing, formatting and proof reading. Using this free service, authors can make their results available to the community, in citable form, before we publish the edited article. We will replace this *Accepted Manuscript* with the edited and formatted *Advance Article* as soon as it is available.

You can find more information about *Accepted Manuscripts* in the [Information for Authors](#).

Please note that technical editing may introduce minor changes to the text and/or graphics, which may alter content. The journal's standard [Terms & Conditions](#) and the [Ethical guidelines](#) still apply. In no event shall the Royal Society of Chemistry be held responsible for any errors or omissions in this *Accepted Manuscript* or any consequences arising from the use of any information it contains.



Journal Name

ARTICLE

Exploring the acid-catalyzed substitution mechanism of $[\text{Fe}_4\text{S}_4\text{Cl}_4]^{2-}$ †

Received 00th January 20xx,
Accepted 00th January 20xx

Thaer M. M. Al-Rammahi^{a,b} and Richard A. Henderson^{a*}

DOI: 10.1039/x0xx00000x

www.rsc.org/

Kinetic studies on the acid-catalyzed substitution reactions of the terminal chloro-ligands in $[\text{Fe}_4\text{S}_4\text{Cl}_4]^{2-}$ by PhS^- in the presence of the acids NHR_3^+ ($\text{R} = \text{Me}, \text{Pr}^n$ or Bu^n) are reported. Although these acids have very similar pK_a s (17.6 – 18.4) the reactions show a variety of different kinetics, some of which are inconsistent with a mechanism involving simple protonation of the cluster followed by substitution of a terminal ligand. The observed behaviour is more consistent with the recently proposed mechanism in which $\text{Fe}-(\mu_3\text{-SH})$ bond elongation/cleavage occurs upon protonation of a $\mu_3\text{-S}$, and suggests that both the acidity and bulk of the acid is important in the protonation step. Other studies have determined the activation parameters (ΔH^\ddagger and ΔS^\ddagger) for both the protonation and substitution steps of the acid-catalyzed substitution reactions of $[\text{Fe}_4\text{S}_4\text{X}_4]^{2-}$ ($\text{X} = \text{Cl}$ or SEt). A significantly negative ΔS^\ddagger is observed for the substitution steps of both clusters indicating associative pathways. This is inconsistent with earlier interpretation of the kinetics of these reactions (based exclusively on the dependence of the rate on the concentration of nucleophile) and indicates that there is no dissociative substitution mechanism and the pathway associated with a zero order dependence on the concentration of PhS^- involves associative substitution with the solvent (MeCN) being the nucleophile.

Introduction

In certain metalloenzymes the sites where substrates bind and are transformed are Fe-S based clusters. These enzymes range from those involved in non-redox transformations (*e.g.* aconitase)¹ to those involved in multi-electron, multi-proton transformations (*e.g.* nitrogenases).² Clearly, these enzymes operate in an aqueous (protic) environment and, in some cases, employ protons as a reactant. Because of the complexity of the biological systems, it is difficult to explore the protonation chemistry of natural Fe-S-based clusters, but studies on synthetic clusters allow the factors which affect both the position and rates of proton transfer in Fe-S-based clusters to be defined. The protonation chemistry of synthetic Fe-S-based clusters has been established, principally, from studies on acid-catalyzed substitution reactions: a reaction whose mechanism has recently been scrutinised.

Kinetic studies on the substitution reactions of the terminal ligands in synthetic Fe-S-based clusters, in the presence of acid, such as NH_4Et_3^+ ($\text{pK}_a = 18.4$ in MeCN),³ show that protonation of the cluster invariably accelerates the rate of substitution.⁴ In a series of studies, the kinetics indicate an acid-catalyzed substitution mechanism involving initial cluster protonation, followed by rate-limiting substitution. The indicated sites of protonation are the core $\mu_3\text{-S}^5$ and early work on $[\text{Fe}_4\text{S}_4\text{X}_4]^{2-}$ (based purely on the dependence of the

rate on the concentration of nucleophile) suggested that the substitution step involves either dissociative ($\text{X} = \text{thiolate}$ or phenolate) or associative ($\text{X} = \text{halide}$) pathways (Fig. 1).^{4,6}

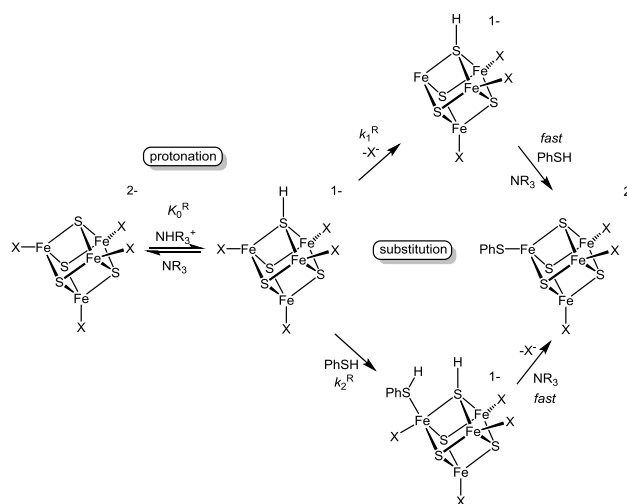


Fig. 1. Early mechanism proposed for the acid-catalyzed substitution reactions of terminal ligands in $[\text{Fe}_4\text{S}_4\text{X}_4]^{2-}$ ($\text{X} = \text{thiolate}$, phenolate or halide). The dissociative (k_1^R) and associative (k_2^R) pathways were suggested based on the kinetics.

However, these acid-catalyzed reactions exhibit some unusual features, which are difficult to reconcile with a simple protonation of the cluster as shown in Fig. 1. The most notable issues have been discussed in detail recently but, briefly, they

^a School of Chemistry, Newcastle University, Newcastle upon Tyne, NE1 7RU, UK. E-mail: richard.henderson@ncl.ac.uk.

^b Department of Chemistry, College of Science, University of Kerbala, Kerbala, Iraq.

† Electronic Supplementary Information (ESI) available: summary of kinetic data for the reactions of $[\text{Fe}_4\text{S}_4\text{Cl}_4]^{2-}$ with PhS^- in the presence of NHR_3^+ ($\text{R} = \text{Me}, \text{Pr}^n$ or Bu^n); kinetic data for the temperature dependences of the reactions of $[\text{Fe}_4\text{S}_4\text{Cl}_4]^{2-}$ and $[\text{Fe}_4\text{S}_4(\text{SEt})_4]^{2-}$. See DOI: 10.1039/x0xx00000x

are as follows.⁷ (i) The rates of proton transfer to Fe-S-based clusters are slower than the diffusion-controlled limit, even for thermodynamically-favourable protonation reactions. (ii) Under conditions where proton transfer is rate-limiting the reaction is not associated with a measurable kinetic isotope effect in studies with deuterated acid. (iii) Protonation of the cluster accelerates the rate of substitution, irrespective of the nature of the terminal ligand (X = thiolate, phenolate or halide), or the kinetics of the substitution step (for X = thiolate or phenolate, rate of substitution independent of the concentration of nucleophile, and for X = halide, rate exhibits a first order dependence on the concentration of nucleophile). (iv) Changes to the ligation and metal composition of cuboidal Fe-S-based cluster modulate the rates of proton transfer in an unusual manner, suggestive of structural changes to the cluster being a significant barrier to protonation. (v) If the mechanism in Fig. 1 operates, the pK_a of the cluster can be calculated from the kinetic data. Such calculations indicate that the pK_a of all Fe-S-based clusters fall in the narrow range 17.9–18.9, independent of overall charge, nuclearity, terminal ligands and cluster composition.

Recent DFT calculations on cubanoid $[\text{Fe}_4\text{S}_4\text{X}_4]^{2-}$ (X = thiolate, phenolate and halide), inspired by earlier calculations on the active site of the Mo-based nitrogenase {a $\text{MoFe}_7\text{S}_9\text{C}(\text{R-homocitrate})$ cluster} indicate that protonation of $\mu_3\text{-S}$ is coupled to cleavage of a Fe-($\mu_3\text{-SH}$) bond (Fig. 2).

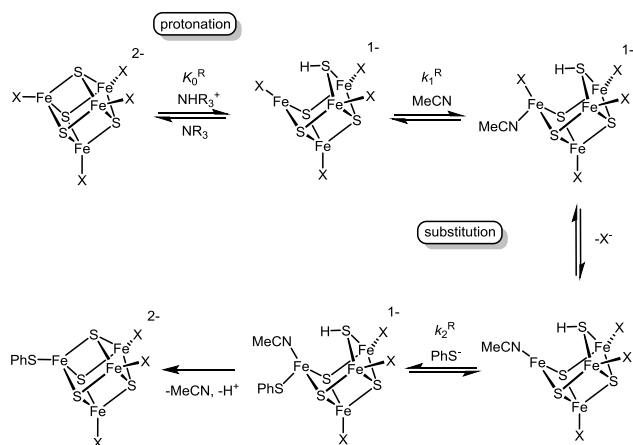


Fig. 2. Recently proposed mechanism for the acid-catalyzed substitution reactions of terminal ligands in $[\text{Fe}_4\text{S}_4\text{X}_4]^{2-}$ (X = thiolate, phenolate or halide), in which Fe-($\mu_3\text{-SH}$) bond cleavage is coupled to

The key steps in the mechanism are as follows. Initial protonation of a $\mu_3\text{-S}$ and concomitant Fe-($\mu_3\text{-SH}$) bond cleavage generates a 3-coordinate Fe, which would appear to be primed as the site of substitution by an associative mechanism. To be consistent with the experimentally observed kinetics, it is suggested that the substitution of X by PhSH (or PhS^-) occurs by two consecutive associative steps which involve initial displacement of X^- by MeCN (the solvent), followed by displacement of coordinated MeCN by PhSH. Depending on the lability of Fe-X, the rate-limiting step can be either displacement of X^- by MeCN (rate independent of concentration of nucleophile), or displacement of coordinated MeCN by PhSH (rate exhibits first order dependence on concentration of nucleophile). All the experimentally

anomalous characteristics observed for the protonation of synthetic Fe-S-based clusters {points (i) – (v) presented above} are explicable using the mechanism shown in Fig. 2.⁷

Irrespective of whether the mechanism is that shown in Fig. 1 or Fig. 2, there are two principal stages: the protonation and the substitution stages. The intimate mechanism of each of these stages is different in the two mechanisms. In this paper we report studies on various cubanoid $[\text{Fe}_4\text{S}_4\text{X}_4]^{2-}$ which explore both the protonation and substitution stages and are designed to distinguish between the mechanisms in Figs. 1 and 2.

Results and discussion

In the presentation that follows we focus initially on exploring the protonation stage. Studies on the reactions between $[\text{Fe}_4\text{S}_4\text{Cl}_4]^{2-}$ with PhS^- in the presence of a series of structurally similar acids, NHR_3^+ (R = Me, Et, Pr^n and Bu^n) show that the rates of the reactions do not correlate with the pK_a s of the acids. This behaviour is inconsistent with the mechanism shown in Fig. 1, but can be rationalised by the mechanism in Fig. 2. In the second part of the presentation we consider the substitution stage. Studies on the temperature dependence of the rate of substitution of $[\text{Fe}_4\text{S}_3(\text{SH})\text{Cl}_4]^-$ (rate exhibits first order dependence on concentration of PhSH) and $[\text{Fe}_4\text{S}_3(\text{SH})(\text{SEt})_4]^-$ (rate is independent of concentration of PhSH) yields ΔH^\ddagger and ΔS^\ddagger for these reactions. A notable feature is that, for both clusters, the substitution step is associated with a negative ΔS^\ddagger , consistent with associative substitution mechanisms. How this observation correlates with the kinetic dependence on the concentration of nucleophile is discussed. Before discussing the kinetics of the acid-catalyzed substitution reactions of $[\text{Fe}_4\text{S}_4\text{X}_4]^{2-}$ we will first outline how the concentrations of acid, base and nucleophile are calculated in mixtures containing NHR_3^+ and PhS^- , and hence how the kinetic data is analysed.

Studying the kinetics of the acid-catalyzed substitution reactions. To study the kinetics of the acid-catalyzed substitution reactions of Fe-S-based clusters the system shown in Fig. 3 was developed. The details of this methodology have been discussed in earlier publications.⁴

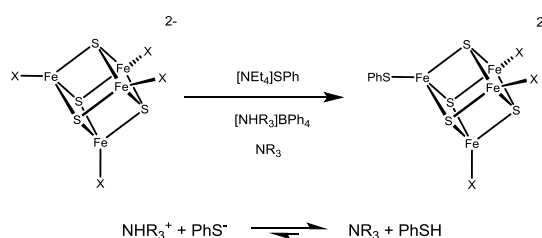


Fig. 3. Components of the system used to study the acid-catalyzed substitution reactions of terminal ligands in $[\text{Fe}_4\text{S}_4\text{X}_4]^{2-}$ (X = thiolate, phenolate or halide), and the protolytic equilibrium which needs to be taken into account when calculating the nature and concentration of acid, base and nucleophile present in MeCN solution.

In this system the cluster is reacted with a mixture containing NHR_3^+ , PhS^- and NR_3 . All the acids employed in the studies reported herein ($\text{R} = \text{Me}, \text{Et}, \text{Pr}^n \text{ or } \text{Bu}^n$) are sufficiently strong acids that the equilibrium between NHR_3^+ and PhS^- lies completely to the right hand side (*vide infra*). Consequently, in the presence of an excess of acid, the species present in solution are NHR_3^+ (the acid), NR_3 (the base) and PhSH (the nucleophile). Furthermore, the concentrations present in solution can be calculated using the simple relationships: $[\text{PhSH}]_e = [\text{PhS}^-]_o$; $[\text{NR}_3]_e = [\text{NR}_3]_o + [\text{PhS}^-]_o$ and $[\text{NHR}_3^+]_e = [\text{NHR}_3^+]_o - [\text{PhS}^-]_o$ (subscript e indicates the equilibrium concentration and subscript o indicates the concentration initially in solution).

Protonation: studies with NHR_3^+ ($\text{R} = \text{Me}, \text{Et}, \text{Pr}^n \text{ or } \text{Bu}^n$). For the mechanism in Fig. 1, the structural integrity of the cluster core remains intact throughout and the rate law for the reaction with $[\text{Fe}_4\text{S}_4\text{Cl}_4]^{2-}$ is that shown in equation (1).⁴ For the mechanism in Fig. 2, the rate law is also equation (1), but in this case K_0^R corresponds to proton transfer and coupled cleavage of a Fe-S bond, and thus, the rates may not correlate with the $\text{p}K_a$ s of the acids, and could also reflect factors which affect the Fe-S cleavage.

$$\text{Rate} = \frac{K_0^R(k_1^R + k_2^R[\text{PhSH}])[\text{Fe}_4\text{S}_4\text{Cl}_4]^{2-}[\text{NHR}_3^+]/[\text{NR}_3]}{1 + K_0^R[\text{NHR}_3^+]/[\text{NR}_3]} \quad (1)$$

If the mechanism shown in Fig. 1 operates, the rate observed with any acid can be calculated, provided the $\text{p}K_a^{\text{NHR}}$ of NHR_3^+ is known.⁶ The value of K_0^R can be calculated using the relationship $K_0^R = K_a^{\text{NHR}}/K_a^{\text{cluster}}$ (for $[\text{Fe}_4\text{S}_4\text{Cl}_4]^{2-}$, $\text{p}K_a^{\text{cluster}} = 18.8$, calculated assuming the mechanism in Fig. 1; from data where NHET_3^+ is the acid).^{4b-4d} Furthermore, the rate constants for the substitution steps for $[\text{Fe}_4\text{S}_4\text{Cl}_4]^{2-}$ are known from earlier studies with NHET_3^+ ,⁵ and are independent of the identity of the acid ($k_1^R = 2.0 \pm 0.3 \text{ s}^{-1}$ and $k_2^R = 1.5 \pm 0.1 \times 10^4 \text{ dm}^3 \text{ mol}^{-1} \text{ s}^{-1}$). If the rate departs from that predicted in this manner, it indicates that the mechanism is not that in Fig. 1.

The kinetics of the reactions between $[\text{Fe}_4\text{S}_4\text{Cl}_4]^{2-}$ and PhS^- have been studied in the presence of a series of acids NHR_3^+ ($\text{R} = \text{Me}, \text{Et}, \text{Pr}^n \text{ and } \text{Bu}^n$). These acids were chosen because they are structurally similar and there is little variation in their $\text{p}K_a$ s. The $\text{p}K_a^{\text{NHR}}$ of the acids (in MeCN) are: NHMe_3^+ ($\text{p}K_a^{\text{NHMe}} = 17.6$); NHET_3^+ ($\text{p}K_a^{\text{NHET}} = 18.4$); NHPr_3^+ ($\text{p}K_a^{\text{NHPr}} = 18.1$); NHBu_3^+ ($\text{p}K_a^{\text{NHBu}} = 18.1$).³

The rate law in equation (1) was originally established from kinetic studies of the reactions between $[\text{Fe}_4\text{S}_4\text{Cl}_4]^{2-}$ and PhS^- in the presence of NHET_3^+ . Analogous studies with NHPr_3^+ also follow equation (1), with the slightly corrected value of K_0^{Pr} (see ESI). However, the kinetics of the similar reactions with NHMe_3^+ and NHBu_3^+ show significant deviations from that predicted by equation (1).

The kinetic data for the reaction between $[\text{Fe}_4\text{S}_4\text{Cl}_4]^{2-}$ and PhS^- in the presence of NHBu_3^+ do not fit equation (1) with the calculated value of $K_0^{\text{Bu}} = 5.0$. This is shown in Fig. 4 (top) where the red dashed curve is the rate defined by equation (1). The experimental data, over a range of different conditions, are shown as various symbols. These experiments were performed under conditions where $[\text{PhSH}]_e = [\text{NHBu}_3^+]_e$ and thus the data in Fig. 4 (top) suggests a rate law exhibiting a first order dependence on $[\text{NHBu}_3^+]_e$ (indicated by the dotted

line). This is confirmed in the plot shown in Fig. 4 (bottom), from which the rate law shown in equation (2) is obtained.

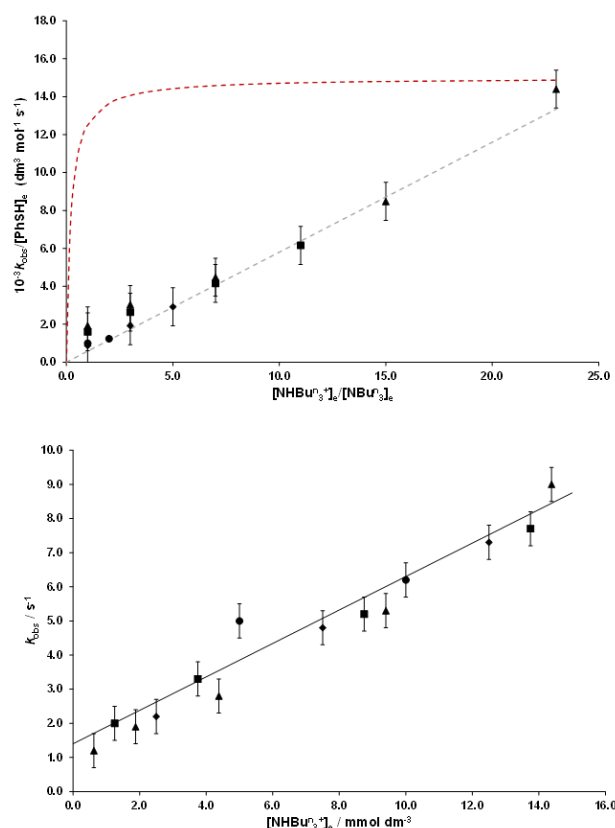


Fig. 4. TOP: Plot of $k_{\text{obs}}/[\text{PhSH}]_e$ versus $[\text{NHBu}_3^+]_e/[\text{NR}_3]_e$ for the reaction of $[\text{Fe}_4\text{S}_4\text{Cl}_4]^{2-}$ (0.2 mmol dm^{-3}) with PhS^- in the presence of NHBu_3^+ in MeCN at $25.0 \text{ }^\circ\text{C}$. The red dashed curve is the rate predicted by Equation (1) using the $\text{p}K_a$ s of NHBu_3^+ and the cluster. The data points correspond to the rate constants at the following concentrations: $[\text{PhSH}]_o = 0.625 \text{ mmol dm}^{-3}$, $[\text{NHBu}_3^+]_o = 0.625 - 15 \text{ mmol dm}^{-3}$ (\blacktriangle); $[\text{PhSH}]_o = 1.25 \text{ mmol dm}^{-3}$, $[\text{NHBu}_3^+]_o = 1.25 - 15 \text{ mmol dm}^{-3}$ (\blacksquare); $[\text{PhSH}]_o = 2.50 \text{ mmol dm}^{-3}$, $[\text{NHBu}_3^+]_o = 2.50 - 15 \text{ mmol dm}^{-3}$ (\blacklozenge); $[\text{PhSH}]_o = 5.0 \text{ mmol dm}^{-3}$, $[\text{NHBu}_3^+]_o = 5.0 - 15 \text{ mmol dm}^{-3}$ (\bullet). BOTTOM: Corresponding plot of k_{obs} versus $[\text{NHBu}_3^+]_e$ (same data as in TOP graph) for the reaction of $[\text{Fe}_4\text{S}_4\text{Cl}_4]^{2-}$ (0.2 mmol dm^{-3}) with PhSH in the presence of NHBu_3^+ in MeCN at $25.0 \text{ }^\circ\text{C}$. $[\text{NHBu}_3^+]_e = [\text{NHBu}_3^+]_o - [\text{PhS}]_o$. The data points correspond to the rate constants at the following concentrations: $[\text{NHBu}_3^+]_o = 0 - 15 \text{ mmol dm}^{-3}$, $[\text{PhS}]_o = 0.625 \text{ mmol dm}^{-3}$ (\blacktriangle); $[\text{NHBu}_3^+]_o = 0 - 15 \text{ mmol dm}^{-3}$, $[\text{PhS}]_o = 1.25 \text{ mmol dm}^{-3}$ (\blacksquare); $[\text{NHBu}_3^+]_o = 0 - 15 \text{ mmol dm}^{-3}$, $[\text{PhS}]_o = 2.5 \text{ mmol dm}^{-3}$ (\blacklozenge); $[\text{NHBu}_3^+]_o = 0 - 15 \text{ mmol dm}^{-3}$, $[\text{PhS}]_o = 5.0 \text{ mmol dm}^{-3}$ (\bullet). The line is that defined by Equation (2).

$$\text{Rate} = \{1.4 + 490[\text{NHBu}_3^+]_e\}[\text{Fe}_4\text{S}_4\text{Cl}_4]^{2-} \quad (2)$$

Equation (2) contains two terms indicating two pathways for substitution: the first term is independent of the concentration of acid and the second term exhibits a first order dependence on the concentration of acid. Both terms are independent of the concentration of nucleophile. Earlier work on the kinetics of the acid-catalysed substitution reactions of $[\text{Fe}_4\text{S}_4\text{Cl}_4]^{2-}$ with PhS^- in the presence of NHET_3^+ showed that, at low concentrations of acid, the uncatalysed substitution pathway becomes evident ($k = 2.0 \pm 0.3 \text{ s}^{-1}$).⁵ This value is in good

agreement with the first term in equation (2). The second term in equation (2) is consistent with a mechanism for acid-catalysed substitution involving rate-limiting proton transfer. Previously, rate-limiting proton transfer of $[\text{Fe}_4\text{S}_4\text{Cl}_4]^{2-}$ has been observed in reactions involving the pyrrolidinium ion (pyrrH^+ , $\text{p}K_a^{\text{pyr}} = 21.5$).³ Proton transfer from pyrrH^+ to cluster is slow presumably because proton transfer is thermodynamically unfavourable.^{8a,9} However, for NHBu_3^+ , $\text{p}K_a^{\text{NHBu}} = 18.1$ and hence proton transfer is more thermodynamically favourable. It seems likely that proton transfer to $[\text{Fe}_4\text{S}_4\text{Cl}_4]^{2-}$ is slow with NHBu_3^+ because of steric factors. The long Bu^n chains are sufficiently bulky to make it difficult for this acid to get close to the cluster for optimal proton transfer (*i.e.* the acidic NH group in NHBu_3^+ is buried by the Bu^n groups). Finally, it should be noted that proton transfer to $[\text{Fe}_4\text{S}_4\text{Cl}_4]^{2-}$ from pyrrH^+ is significantly faster ($k_0^{\text{pyr}} = 2.1 \times 10^4 \text{ dm}^3 \text{ mol}^{-1} \text{ s}^{-1}$)⁸ than from NHBu_3^+ ($k_0^{\text{NHBu}} = 490 \text{ dm}^3 \text{ mol}^{-1} \text{ s}^{-1}$). However, it is difficult to interpret this variation in rates because of the different reasons pyrrH^+ and NHBu_3^+ transfer protons slowly to the cluster.

The kinetic data for the reaction between $[\text{Fe}_4\text{S}_4\text{Cl}_4]^{2-}$ and PhS^- , in the presence of NHMe_3^+ are shown in Fig. 5. The red dashed curve shows the dependence of $k_{\text{obs}}/[\text{PhSH}]$ on $[\text{NHMe}_3^+]_e/[\text{NMe}_3]_e$ predicted by equation (1), using $K_0^{\text{Me}} = 15.9$ (calculated from the $\text{p}K_a$ s of the cluster and NHMe_3^+). Obviously, the experimental data does not fit the predicted rate, and the fit to the experimental data is the solid curve which is defined by equation (3).

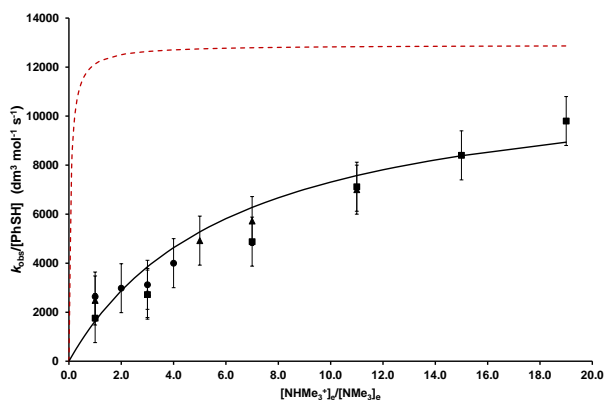


Fig. 5. Plot of $k_{\text{obs}}/[\text{PhSH}]_e$ versus $[\text{NHMe}_3^+]_e/[\text{NMe}_3]_e$ for the reaction of $[\text{Fe}_4\text{S}_4\text{Cl}_4]^{2-}$ (0.2 mmol dm^{-3}) with PhS^- in the presence of NHMe_3^+ in MeCN at $25.0 \text{ }^\circ\text{C}$. The red dashed curve is the rate predicted by Equation (1) using the $\text{p}K_a$ s of NHMe_3^+ (17.6) and the cluster (0.2 mmol dm^{-3}). The data points correspond to the rate constants at the following concentrations: $[\text{PhS}^-]_0 = 1.25 \text{ mmol dm}^{-3}$, $[\text{NHMe}_3^+]_0 = 2.5 - 25 \text{ mmol dm}^{-3}$ (\blacksquare); $[\text{PhS}^-]_0 = 2.5 \text{ mmol dm}^{-3}$, $[\text{NHMe}_3^+]_0 = 2.5 - 25 \text{ mmol dm}^{-3}$ (\blacktriangle); $[\text{PhS}^-]_0 = 5.0 \text{ mmol dm}^{-3}$, $[\text{NHMe}_3^+]_0 = 2.5 - 25 \text{ mmol dm}^{-3}$ (\bullet). The solid curve is that defined by Equation (3).

$$\text{Rate} = \frac{(1.9 \times 10^3)[\text{Fe}_4\text{S}_4\text{Cl}_4]^{2-}[\text{PhSH}][\text{NHMe}_3^+]_e/[\text{NMe}_3]_e}{1 + 0.16[\text{NHMe}_3^+]_e/[\text{NMe}_3]_e} \quad (3)$$

The rate law in equation (3) is clearly of the same form as equation (1),^{4,6} and comparison of equations (1) and (3) gives $K_0^{\text{Me}} = 0.16$ and $k_2^{\text{Me}} = 1.2 \pm 0.1 \times 10^4 \text{ dm}^3 \text{ mol}^{-1} \text{ s}^{-1}$. Thus, at high values of $[\text{NHMe}_3^+]_e/[\text{NMe}_3]_e$, the rate is independent of

$[\text{NHMe}_3^+]_e/[\text{NMe}_3]_e$ and is identical to that observed with NHMe_3^+ and NHPPr_3^+ ($k_2^{\text{R}} = 1.2 \pm 0.1 \times 10^4 \text{ dm}^3 \text{ mol}^{-1} \text{ s}^{-1}$), corresponding to substitution of the protonated cluster, $[\text{Fe}_4\text{S}_3(\text{SH})\text{Cl}_4]^+$. However, at low values of $[\text{NHMe}_3^+]_e/[\text{NMe}_3]_e$, the rate is appreciably slower than predicted by equation (1). Although equation (3) is of the same form as equation (1), it is not consistent with the mechanism in Fig. 1 because the value of $K_0^{\text{Me}} = 0.16$ is significantly different to the value $K_0^{\text{Me}} = 15.9$ calculated from the $\text{p}K_a$ s of the cluster and NHMe_3^+ .¹⁰

The studies with NHMe_3^+ indicate that protonation of $[\text{Fe}_4\text{S}_4\text{Cl}_4]^{2-}$ does not involve just the simple addition of a proton to the cluster. For the mechanism in Fig. 2, protonation of the cluster involves both proton transfer to a $\mu_3\text{-S}$ and $\text{Fe}-(\mu_3\text{-SH})$ bond cleavage/elongation. Consequently, we need to consider how changes to NHR_3^+ might affect both the proton transfer and the $\text{Fe}-(\mu_3\text{-SH})$ bond elongation.

Of all the acids investigated in this study, it is notable that NHMe_3^+ is the least bulky. We suggest that both the acidity and the bulk of the acid are significant in protonating $[\text{Fe}_4\text{S}_4\text{Cl}_4]^{2-}$. For the mechanism in Fig. 2, as NHR_3^+ hydrogen bonds to a $\mu_3\text{-S}$ (in preparation for proton transfer), a $\text{Fe}-(\mu_3\text{-S})$ bond elongates in concert (Fig. 6).⁷ It seems likely that the incipient cluster disruption is facilitated by more bulky (longer R) groups of the acid because the longer the R groups the more they will interfere with the terminal chloro-ligand of $[\text{Fe}_4\text{S}_4\text{Cl}_4]^{2-}$ and, in order to relieve congestion, the $\text{Fe}-(\mu_3\text{-SH})$ will elongate. Consequently, the transition states for proton transfer with the series of acids, NHR_3^+ ($\text{R} = \text{Me}, \text{Et}, \text{Pr}^n$ and Bu^n) are subtly different, with the interference between the R groups and the chloro-ligands increasing as the size of R increases. With NHBu_3^+ , the interference between the Bu^n groups and chloro-ligands is so severe that proton transfer becomes sufficiently slow that it is rate limiting.

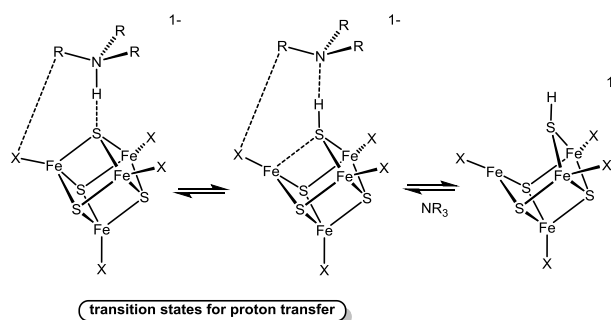


Fig. 6. Representation of the transition state for proton transfer from NHR_3^+ to $[\text{Fe}_4\text{S}_4\text{X}_4]^{2-}$ indicating how interference between the terminal X group and the R group of the acid could facilitate $\text{Fe}-(\mu_3\text{-SH})$ elongation/cleavage. It seems likely that the interference is most significant for the endo conformer of $\{[\text{Fe}_4\text{S}_4\text{X}_4] \dots \text{NHR}_3\}^+$.

Substitution: effect of temperature. The rates of the acid-catalysed substitution reactions of $[\text{Fe}_4\text{S}_4\text{X}_4]^{2-}$ are either independent of the concentration of nucleophile ($\text{X} = \text{thiolate}$ or phenolate) or exhibit a first order dependence on the concentration of nucleophile ($\text{X} = \text{halide}$). The interpretation of these dependences is different for the mechanisms shown in Figs. 1 and 2. For the mechanism in Fig. 1 it has been proposed that the different dependences on the concentrations of nucleophile are due to different mechanisms of substitution

(i.e. for X = RS or PhO, substitution occurs by a dissociative pathway but for X = halide, substitution occurs by an associative pathway).^{5,6} For the mechanism in Fig. 2, the transient formation of a 3-coordinate Fe suggests this site is primed for nucleophilic attack and that an associative mechanism will always prevail. Consequently, for this mechanism, it has been suggested that the substitution of all $[\text{Fe}_4\text{S}_3(\text{SH})\text{X}_4]^-$ involve initial attack of MeCN (solvent), and the coordinated MeCN is subsequently displaced by PhSH.⁷ When X = RS or PhO, displacement of coordinated X by MeCN is rate limiting, but for the more labile $[\text{Fe}_4\text{S}_3(\text{SH})\text{Cl}_4]^-$, displacement of X = Cl by MeCN is rapid and the displacement of coordinated MeCN by PhSH is rate-limiting. In order to probe further the intimate mechanisms of the substitution step in the acid-catalysed substitution reactions we have investigated the temperature dependence of the reactions to determine ΔH^\ddagger and ΔS^\ddagger .

The reactions whose temperature dependences are reported in this paper are summarized in Table 1. In all cases, the temperature dependences of the reactions were measured over the temperature range 15 – 35 °C (see ESI).

Table 1. Temperature dependent studies. Kinetic characteristics for reactions of $[\text{Fe}_4\text{S}_4\text{X}_4]^{2-}$ (X = Cl or SET) with PhSH in the presence of acids.

cluster	acid	kinetics ^a
$[\text{Fe}_4\text{S}_4\text{Cl}_4]^{2-}$	NHBu_3^+	$k_{\text{obs}} = k_0^{\text{NHBu}_3^+} [\text{NHBu}_3^+]$ rate-limiting protonation
$[\text{Fe}_4\text{S}_4\text{Cl}_4]^{2-}$	NHET_3^+	$k_{\text{obs}} = K_0^{\text{NHET}_3^+} k_2^{\text{NHET}_3^+} [\text{PhSH}]_e / (1 + K_0^{\text{NHET}_3^+} A)$ rate-limiting substitution first order dependence on [PhSH]
$[\text{Fe}_4\text{S}_4(\text{SET})_4]^{2-}$	NHET_3^+	$k_{\text{obs}} = K_0^{\text{NHET}_3^+} k_1^{\text{NHET}_3^+} A / (1 + K_0^{\text{NHET}_3^+} A)$ rate-limiting substitution rate independent of [PhSH]

footnote: ^a A = $[\text{NHET}_3^+] / [\text{NET}_3]$

For the reaction of $[\text{Fe}_4\text{S}_4\text{Cl}_4]^{2-}$ with PhS^- in the presence of NHBu_3^+ , where proton transfer from the acid to $[\text{Fe}_4\text{S}_4\text{Cl}_4]^{2-}$ is rate-limiting, $\Delta H^\ddagger = 0.26 \pm 0.1 \text{ kcal mol}^{-1}$ and $\Delta S^\ddagger = -19.1 \pm 2.0 \text{ cal deg}^{-1} \text{ mol}^{-1}$. The Eyring plot for this reaction is shown in Fig. 7. The Eyring plots for the other systems discussed below are shown in ESI. These values of ΔH^\ddagger and ΔS^\ddagger are similar to those measured earlier for the same cluster reacting with Br^- in the presence of pyrrH^+ ($\Delta H^\ddagger = 0.45 \pm 0.2 \text{ kcal mol}^{-1}$ and $\Delta S^\ddagger = -47.0 \pm 5.0 \text{ cal deg}^{-1} \text{ mol}^{-1}$),^{8b} and are consistent with proton transfer where the transition state involves prior association (hydrogen bonding) of the acid with the cluster (i.e. a small ΔH^\ddagger and negative ΔS^\ddagger).¹¹ The larger value of ΔH^\ddagger and more negative ΔS^\ddagger associated with the reactions of pyrrH^+ is presumably a consequence of the weaker acidity of this acid, resulting in a weaker (longer) hydrogen bond in the transition state. A common feature of the proton transfer reactions of synthetic Fe-S-based clusters is a small ΔH^\ddagger .^{8b,8e} Whilst small ΔH^\ddagger are often associated with diffusion-controlled reactions, the rate constants for proton transfer to Fe-S-based clusters indicate that this is not the case for these reactions.

The reaction between $[\text{Fe}_4\text{S}_4\text{Cl}_4]^{2-}$ and PhS^- in the presence of NHET_3^+ exhibits a non-linear dependence on the ratio $[\text{NHET}_3^+]_e / [\text{NET}_3]_e$ (see Table 1 and ESI).⁵ Consequently, measuring the temperature dependence over a range of $[\text{NHET}_3^+]_e / [\text{NET}_3]_e$ allows separate determination of the activation parameters for the protonation step (K_0^{R}) and the

substitution step (k_2^{R}). For the protonation of $[\text{Fe}_4\text{S}_4\text{Cl}_4]^{2-}$, $\Delta H^\circ = 0.03 \pm 0.05 \text{ kcal mol}^{-1}$ and $\Delta S^\circ = -25.1 \pm 5.0 \text{ cal deg}^{-1} \text{ mol}^{-1}$, and for the substitution step, $\Delta H^\ddagger = 0.37 \pm 0.1 \text{ kcal mol}^{-1}$ and $\Delta S^\ddagger = -16.6 \pm 2.0 \text{ cal deg}^{-1} \text{ mol}^{-1}$. A notable feature is the negative ΔS^\ddagger for the substitution step, which is indicative of an associative mechanism. This conclusion correlates with the kinetics which exhibit a first order dependence on the concentration of PhSH.

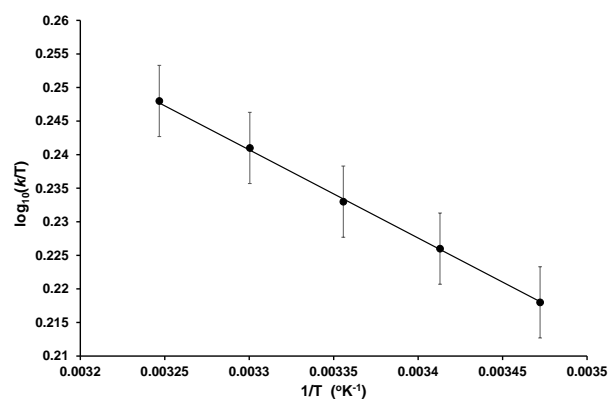


Fig. 7. Eyring plot the Reaction of $[\text{Fe}_4\text{S}_4\text{Cl}_4]^{2-}$ (0.2 mmol dm⁻³) with PhSH in the presence of NHBu_3^+ in MeCN.

A mechanistically more revealing result comes from studies on the temperature dependence of the reaction between $[\text{Fe}_4\text{S}_4(\text{SET})_4]^{2-}$ and PhS^- in the presence of NHET_3^+ . The slowness of this reaction makes it difficult to study the temperature dependence over a wide range of $[\text{NHET}_3^+]_e / [\text{NET}_3]_e$. Consequently, the temperature dependence has been studied only when $[\text{NHET}_3^+]_e / [\text{NET}_3]_e = 9.0$. Under these conditions all of the cluster is protonated and the measured activation parameters ($\Delta H^\ddagger = 0.55 \pm 0.15 \text{ kcal mol}^{-1}$ and $\Delta S^\ddagger = -22.9 \pm 2.0 \text{ cal deg}^{-1} \text{ mol}^{-1}$) correspond to the substitution of $[\text{Fe}_4\text{S}_3(\text{SH})(\text{SET})_4]^-$. Of particular note is the negative value of ΔS^\ddagger . This is inconsistent with the substitution step occurring by a dissociative mechanism, as suggested by the kinetics (i.e. a zero order dependence on the concentration of nucleophile, see Table 1).^{6a} The negative ΔS^\ddagger is indicative of an associative mechanism. The negative ΔS^\ddagger , but zero order dependence on the concentration of nucleophile, is consistent with an associative substitution mechanism for $[\text{Fe}_4\text{S}_3(\text{SH})(\text{SET})_4]^-$, involving the solvent (MeCN) as nucleophile. For either mechanism (Fig. 1 or 2), this would involve displacement of a EtS ligand by MeCN, but for the mechanism in Fig. 1 the process occurs at a tetrahedral Fe in an intact cubanoid cluster, whilst in the mechanism in Fig. 2 the displacement occurs at a 3-coordinate Fe after protonation has disrupted the structure of the cluster. Whilst the values of ΔH^\ddagger and ΔS^\ddagger observed in this system cannot distinguish between these two possibilities, establishing that the substitution step in acid-catalysed substitution reactions of Fe-S-based clusters occur by an associative mechanism (irrespective of whether the rate exhibits a zero order or first order dependence on the concentration of nucleophile) is consistent with the mechanism shown in Fig. 2.

Conclusions

Earlier studies on the mechanism of the acid-catalyzed substitution reactions of cubanoid $[\text{Fe}_4\text{S}_4\text{X}_4]^{2-}$ ($\text{X} = \text{thiolate}$, phenolate or halide) had identified some unusual characteristics for these reactions associated with their protonation. As pointed out recently, these characteristics are not easily explained by simple protonation of the cluster (Fig. 1).^{7a} Recently, DFT calculations have indicated that upon protonation of a $\mu_3\text{-S}$ there is elongation/cleavage of the $\text{Fe}-(\mu_3\text{-SH})$ bond (Fig. 2), and this new mechanism rationalises all the unusual observations about protonation of Fe-S -based clusters.⁷ In this paper we have reported further studies on the acid-catalyzed substitution reactions of $[\text{Fe}_4\text{S}_4\text{Cl}_4]^{2-}$. These studies explored the two main stages of the reaction (protonation of the cluster and substitution of a terminal ligand) with the aim of distinguishing between the mechanisms in Figs. 1 and 2. Although the results do not unambiguously establish that protonation disrupts the cluster core, they do identify further peculiarities in the protonation reactions of Fe-S clusters which are, on balance, more consistent with the mechanism shown in Fig. 2.

To explore the protonation step, the kinetics of the acid-catalyzed substitution reactions of $[\text{Fe}_4\text{S}_4\text{Cl}_4]^{2-}$ with PhS^- in the presence of a series of similar acids, NHR_3^+ ($\text{R} = \text{Me}$, Et , Pr^n or Bu^n) with very similar pK_a s have been studied. The crucial result from these studies is that the rate of the reactions cannot be predicted on the basis of the acidities of NHR_3^+ , but rather both the acid strength and the bulk of the R group appear to be important in the protonation step. This observation is inconsistent with the mechanism in Fig. 1, but is reconcilable with the mechanism involving cluster disruption (Fig. 2).

Further studies (Table 1) explored the mechanism of the substitution step. The activation parameters (ΔH^\ddagger and ΔS^\ddagger) for the reactions of $[\text{Fe}_4\text{S}_3(\text{SH})(\text{SET})_4]^-$ with PhS^- (rate of reaction independent of concentration of nucleophile) and $[\text{Fe}_4\text{S}_3(\text{SH})\text{Cl}_4]^-$ (rate exhibits first order dependence on concentration of nucleophile) have been measured. In both reactions, ΔS^\ddagger is negative which indicates that the mechanism of substitution is associative. For the reaction of $[\text{Fe}_4\text{S}_3(\text{SH})(\text{SET})_4]^-$, the negative ΔS^\ddagger , but independence of the rate on the concentration of nucleophile, can be rationalised by an associative, rate-limiting displacement of thiolate by MeCN (solvent), as suggested for the mechanism in Fig. 2.

Experimental

All manipulations in both the synthetic and kinetic aspects of this work were performed under an atmosphere of dinitrogen using Schlenk or syringe techniques, as appropriate. The following chemicals were purchased from Sigma-Aldrich and used as received without any further purifications: anhydrous FeCl_3 , thiophenol, sulfur, $[\text{NHMe}_3]\text{Cl}$, NPr^n_3 , NBu^n_3 and NaBPh_4 . CD_3CN was purchased from Goss Scientific and used as received. $[\text{NBu}_4]_2[\text{Fe}_4\text{S}_4\text{Cl}_4]^{12}$ and $[\text{NEt}_4]\text{SPh}^{13}$ were prepared by the literature methods.

Preparation of $[\text{NHMe}_3]\text{BPh}_4$. $[\text{NHMe}_3]\text{Cl}$ (2.39 g, 25 mmol) was dissolved in the minimum volume of methanol (*ca* 10 ml) and then filtered through celite. NaBPh_4 (8.55 g, 25 mmol) was also dissolved in minimum of methanol (*ca* 10 ml), and then dripped through celite into the $[\text{NHMe}_3]\text{Cl}$ solution. The mixture was left to stand

overnight and a white precipitate resulted. The product was collected by filtration, then was washed by a large volume of distilled water (*ca* 2 liters). The solid precipitate was also washed by small volume of methanol (25 ml) and dried *in vacuo*.

^1H NMR spectrum of $[\text{NHMe}_3][\text{BPh}_4]$ in CD_3CN : δ 2.68 (singlet, intensity = 9, CH_3), 6.83-7.3 (multiplet, intensity = 20, BPh_4).

Preparation of $[\text{NHR}_3]\text{BPh}_4$ ($\text{R} = \text{Pr}^n$ or Bu^n). A method analogous to that reported for $[\text{NHET}_3][\text{BPh}_4]^{14}$ was used to prepare $[\text{NHR}_3][\text{BPh}_4]$ ($\text{R} = \text{Pr}^n$ and Bu^n).

The required amount of NR_3 ($\text{R} = \text{Pr}^n$, 19 ml; $\text{R} = \text{Bu}^n$, 23.8 ml, 100 mmol) was added to THF (100 ml) under an atmosphere of dinitrogen. Methanol (4.05 ml, 100 mmol) was then added to the amine solution, followed by Me_3SiCl (12.7 ml, 100 mmol) with stirring. A white precipitate is immediately formed, and the mixture was stirred for a further 0.5 h. The $[\text{NHR}_3]\text{Cl}$ product was then filtered and washed with the minimum volume of THF then dried *in vacuo*. The dry $[\text{NHR}_3]\text{Cl}$ ($\text{R} = \text{Pr}^n$, 2.7 g; $\text{R} = \text{Bu}^n$, 3.32 g, 15 mmol) was dissolved in the minimum of methanol (*ca* 30 ml), then filtered through celite. The NaBPh_4 (5.2 g, 15 mmol) was dissolved in the minimum of methanol (*ca* 20 ml), and then passed through celite to drip slowly into the solution of $[\text{NHR}_3]\text{Cl}$. The solution was left to stand overnight and a white solid was formed. The solid was collected by filtration, then washed with a large volume of distilled water (*ca* 2 liters). The solid was finally washed with methanol (50 ml) and dried *in vacuo*.

The ^1H NMR spectra of $[\text{NHR}_3]\text{BPh}_4$ in CD_3CN . $[\text{NHPr}^n_3]\text{BPh}_4$: δ 0.93 (triplet, intensity = 9, $J_{\text{HH}} = 7.4$ Hz, CH_3), 1.58-1.68 (multiplet, intensity = 6, CH_2), 2.9-3.0 (multiplet, intensity = 7, CH_2), 6.78-7.3 (multiplet, intensity = 20, BPh_4); $[\text{NHBu}^n_3]\text{BPh}_4$: δ 0.94 (triplet, intensity = 9, $J_{\text{HH}} = 7.3$ Hz, CH_3), 1.33 (hextet, intensity = 6, $J_{\text{HH}} = 7.4$ Hz, CH_2), 1.54-1.62 (multiplet, intensity = 6, CH_2), 2.9-3.0 (multiplet, intensity = 6, CH_2), 6.84-7.33 (multiplet, intensity = 20, BPh_4).

Kinetic studies. All kinetic studies were performed using an Applied Photophysics SX.18 MV stopped-flow spectrophotometer, modified to handle air-sensitive solutions, connected to a RISC computer. The temperature was maintained using a Grant LTD6G thermostat tank with combined recirculating pump. The experiments were performed at 25.0 °C and the wavelength used was $\lambda = 550$ nm. All kinetics were studied in MeCN . The MeCN was dried over CaH_2 and distilled immediately prior to use.

The solutions of $[\text{NBu}_4]_2[\text{Fe}_4\text{S}_4\text{Cl}_4]$ and reagents (NHR_3^+ and PhS^-) were prepared under an atmosphere of dinitrogen. The diluted solutions containing mixtures of NHR_3^+ and PhS^- were prepared from freshly prepared stock solutions. All solutions were used within 1 h.

Under all conditions, the stopped-flow absorbance-time traces were biphasic and were an excellent fit to two exponentials, indicating a first-order dependence on the concentration of the cluster. The dependences on the concentrations of NHR_3^+ , NR_3 and PhSH were determined from analysis of the appropriate graphs as explained in the text.

Acknowledgements

T. Al-Rammahi. thanks the Higher Committee for Education Development in Iraq and Iraqi Ministry of Higher Education and Scientific Research for a studentship.

Notes and references

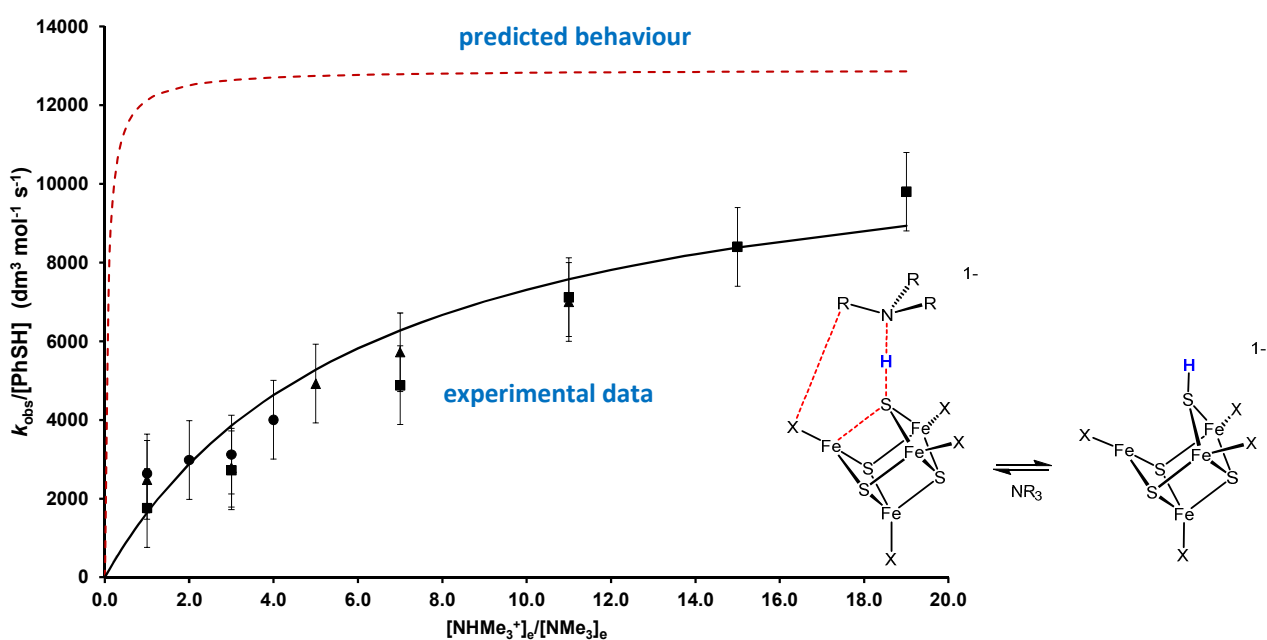
- (a) R. H. Holm, P. Kennepohl and E. I. Solomon, *Chem. Rev.*, 1996, **96**, 2239; (b) H. Beinert, M. C. Kennedy and C. D. Stout, *Chem. Rev.*, 1996, **96**, 2335.
- (a) B. Burgess and D. J. Lowe, *Chem. Rev.*, 1996, **96**, 2983; (b) J. B. Howard and D. C. Rees, *Chem. Rev.*, 1996, **96**, 2965; (c) T. Spatzal, M. Akoyoglu, L. Zhang, S. L. A. Andrade, E. Schleicher, S. Weber, D. C. Rees and O. Einsle, *Science*, 2011, **334**, 940; (d) D. Lukoyanov, Z-Y Yang, N. Khadka, D. R. Dean, L. C. Seefeldt and B. M. Hoffman, *J. Am. Chem. Soc.*, 2015, **137**, 3610.
- K. Izutsu, *Acid-Base Dissociation Constants in Aprotic Solvents*, 1990, Blackwell Scientific, Oxford, UK.
- (a) G. R. Dukes and R. H. Holm, *J. Am. Chem. Soc.*, 1975, **97**, 528; (b) R. A. Henderson, *Chem. Rev.*, 2005, **105**, 2365; (c) R. A. Henderson, *Coord. Chem. Rev.*, 2005, **249**, 1841; (d) R. A. Henderson, *Bioinorg. React. Mech.*, 2012, **8**, 1.
- R. A. Henderson and K. E. Oglieve, *J. Chem. Soc., Chem. Commun.*, 1994, 377.
- (a) R. A. Henderson and K. E. Oglieve, *J. Chem. Soc., Dalton Trans.*, 1993, 1467; (b) R. A. Henderson and K. E. Oglieve, *J. Chem. Soc., Dalton Trans.*, 1993, 1473.
- (a) A. Alwaaly, I. Dance and R. A. Henderson, *Chem. Commun.*, 2014, **50**, 4799; (b) I. Dance and R. A. Henderson, *Dalton Trans.*, 2014, **43**, 16213; (c) I. Dance, *Dalton Trans.*, 2015, **44**, 4707.
- (a) R. A. Henderson and K. E. Oglieve, *J. Chem. Soc., Dalton Trans.*, 1999, 3927; (b) J. Bell, A. J. Dunford, E. Hollis and R. A. Henderson, *Angew. Chem. Int. Ed.*, 2003, **42**, 1149; (c) K. Bates and R. A. Henderson, *Inorg. Chem.*, 2008, **47**, 5850; (d) B. Garrett and R. A. Henderson, *Dalton Trans.*, 2010, **39**, 4586; (e) K. Bates, B. Garrett and R. A. Henderson, *Inorg. Chem.*, 2007, **46**, 11145.
- R. P. Bell, *The Proton in Chemistry*, 2nd edition, Chapman Hall, London, 1973, p195, and references therein.
- The value of K_0^{Me} would only be consistent with the data for NHEt_3^+ and NHPr_3^+ if for NHMe_3^+ $\text{p}K_{\text{a}} = 19.6$. This value is two $\text{p}K_{\text{a}}$ units different from the literature value ($\text{p}K_{\text{a}}^{\text{Me}} = 17.6$).³ It is unreasonable that the literature value of $\text{p}K_{\text{a}}^{\text{Me}}$ is so much in error, if for no other reason than it would mean the $\text{p}K_{\text{a}}$ of NHMe_3^+ was very different to other NHR_3^+ .
- (a) W. J. Albery, *Annu. Rev. Phys. Chem.*, 1980, **31**, 227; (b) W. J. Albery, *Faraday Discuss. Chem. Soc.*, 1982, **74**, 245.
- (a) K. S. Hagen, J. G. Reynolds and R. H. Holm, *J. Am. Chem. Soc.*, 1981, **103**, 4054; (b) G. B. Wong, M. A. Bobrick and R. H. Holm, *Inorg. Chem.*, 1978, **17**, 578.
- R. E. Palermo, P. P. Power and R. H. Holm, *Inorg. Chem.*, 1982, **21**, 173.
- J. R. Dilworth, R. A. Henderson, P. Dahlstrom, T. Nicholson and J. A. Zubieta, *J. Chem. Soc., Dalton Trans.*, 1987, 529.

Exploring the acid-catalyzed substitution mechanism of $[\text{Fe}_4\text{S}_4\text{Cl}_4]^{2-}$

Thaer M. M. Al-Rammahi and Richard A. Henderson

ABSTRACTS

Graphical Abstract



Textual Abstract

Kinetic studies focussing on either the protonation or substitution step of the acid catalyzed substitution reactions of $[\text{Fe}_4\text{S}_4\text{Cl}_4]^{2-}$ support a mechanism involving concomitant cluster protonation and Fe-(μ_3 -SH) bond cleavage.